*Journal of Fluorescence, Vol. 13, No. 4, July 2003 (© 2003)*

# DNA Vector Polyethyleneimine Affects Cell pH and Membrane Potential: A Time-Resolved Fluorescence Microscopy Study

**Ira,[1] Y. Mély,[2] and G. Krishnamoorthy[1,3]**

*Received February 22, 2003; accepted April 9, 2003*

Polyethyleneimine (PEI) is one of the very efficient nonviral vectors being developed and tested for artificial gene transfer into target cells. One of its serious limitations is the significant cytotoxicity of the large amounts of free PEI in the mixtures of DNA and PEI used for transfection. To further investigate the cellular effects of free PEI, we have analyzed the PEI-induced alterations of various cell parameters such as membrane heterogeneity and fluidity, cytoplasmic pH, and plasma membrane potential in a variety of cells such as Swiss 3T3 fibroblast, Chinese hamster ovary, insect cells SF9, plant cell line BY2, and *Saccharomyces cerevisae*. Fluorescence probes such as Nile red, SNARF-1, and cyanine dye $DiSC_2(3)$, coupled with the technique of picosecond time-resolved fluorescence microscopy, were used in estimating the above-mentioned cell parameters. It was found that the cell membranes were largely unperturbed by PEI. However, the cytoplasmic pH showed an increase of ~0.1–0.4 units when the cells were treated with PEI. The plasma membrane potential was found to be depolarized in *S. cerevisae* and Swiss 3T3 cells. These results suggest that the cytotoxic effects of PEI may partly originate from inhibition of regulation of cytoplasmic pH and plasma membrane potential. Further, it is proposed that the resultant cell alterations favors the transfection process.

**KEY WORDS:** Gene therapy; polyethyleneimine; cytoplasmic pH; plasma membrane potential; time-resolved fluorescence microscopy; SNARF-1; $DiSC_2(3)$.

## INTRODUCTION

Delivery of genes into cells is a fundamental technology necessary for basic research in molecular biology as well as medical applications such as gene therapy. Progress in this technology relies upon the development of suitable carriers (vectors) that can transport intact DNA molecules into the nucleus of the host cell. Vectors derived from viral sources are efficient carriers resulting in high levels of transfection [1,2]. However, their use is limited by the induction of immune responses and virus-associated pathogenicity [1,2]. To circumvent these limitations, a large variety of synthetic vectors such as cationic lipids and polyamines have been introduced [3–17]. These nonviral vectors, however, are generally less efficient than viral vectors and require various types of modifications to increase their efficiency [12,13,18] and direct them toward appropriate target locations [19]. Polyethyleneimine (PEI) class of vectors is among the most efficient nonviral vectors developed recently [5,8]. PEI not only have greater efficiency *in vitro*, they have also been shown to have *in vivo* applications [5,9–11]. From gene transfer experiments with PEI-DNA complex in mouse brain it appears that

[1] Department of Chemical Sciences, Tata Institute of Fundamental Research Homi Bhabha Road, Mumbai 400 005, India.
[2] Laboratoire 'Pharmacologie et physico-chimie des interactions cellulaires et moleculaires' UMR 7034 du CNRS, Faculté de Pharmacie Université Louis Pasteur de Strasbourg, 74 Route du Rhin, 67401 Illkirch, France.
[3] To whom all correspondence should be addressed. Fax: +91-22-2280-4610, +91-22-2280-4611. E-mail: gk@tifr.res.in



1053-0509/03/0700-0339/0 © 2003 Plenum Publishing Corporation

PEI is an ideal vector for *in vivo* gene transfer into the mammalian brain at different stages of development [10]. The relatively high efficiency of transfection induced by PEI arises probably as a result of a variety of factors such as high buffering capacity (and hence protection of DNA), capacity to become liberated from endosomes into the cytoplasm, small size (<100 nm) of the complexes [4,5,13], stability of the complex under physiologic conditions, and the ability of translocation into nucleus. Further, the ease with which PEI can be chemically modified is advantageous in conjugating various recognition sequences for specific targeting [13,19].

One of the serious limitations of using transfection agents is their toxicity to cells [20,21]. This toxicity arises as a result of the use of high concentrations of agents needed for appreciable levels of transfection. Moreover, recent work by fluorescence correlation spectroscopy has shown that mixtures of DNA and PEI giving efficient transfection contain about 85% of PEI is in the free form [23]. Further it has been shown by confocal imaging [24,25] and tracer analysis [26] that apart from the PEI-DNA complex, free PEI is also endocytosed. To further investigate the effects of the large amounts of free PEI in transfection protocols using PEI, we have evaluated in the present work, the alteration of several cell parameters, such as cytoplasmic pH, and membrane potential in a variety of cell types challenged with PEI. Fluorescence probes coupled with the technique of time-resolved fluorescence microscopy was used in these measurements. Our technique [27–29] is capable of estimating very small changes in the cytoplasmic pH and membrane potential within a single cell. Our results show that internalization of PEI leads to an increase in intracellular pH in all the various animal and plant cell types studied. Transmembrane potential measurements show that the plasma membrane gets depolarized subsequent to the treatment with PEI.

## EXPERIMENTAL

### Materials

The following cell lines were used in this work: Tobacco BY2 cell line, Swiss 3T3 fibroblasts, SF 9 cell line (from the insect *Spodoptera frugiperda*), yeast (*Saccharomyces cerevisae*) (e.g., 103) cells, and Chinese hamster ovary (CHO) cells. PEI (Average mol. wt. 25 kDa) was from Aldrich Chemical Co. Carboxy SNARF-1 acetoxy methyl ester and $DiSC_2(3)$ were obtained from Molecular Probes Inc. Nile red and valinomycin were from Sigma Chemical Co. (St. Louis, MO, USA).

### Methods

Incubation of the cells with PEI was performed at room temperature (25°C) in a serum-free medium. Details about typical concentrations of PEI used for each cell line along with information about the number of cells and volumes of cell suspensions are given in Table I. In general, the concentration (by total N) of PEI was in the range of 200 μ*M* to 1.4 m*M*. For cell membrane dynamics studies the cells were labeled with Nile red by incubating with ~0.05 m*M* Nile red in PBS for 15–20 min. The excess dye was then washed off with PBS. For cell pH measurements cell-permeant ester (cSNARF-1 AM) of the pH probe (5- and 6-carboxy SNARF-1) was loaded onto cells by adding the dye to the cell suspension (final concentration of 20 μ*M*) at room temperature for 1 h. The cell suspension was then washed with buffer (phosphate buffered saline, pH 7.5; or Murashige and Skoog basal salts with minimal organics, pH 5.8, in case of BY2 cells) to remove external dye. cSNARF-1 AM ester gets hydrolyzed in the cell by nonspecific esterases to give free acid, which is cell impermeant. In experiments for the estimation of membrane potential in vesicle membranes, soybean phospholipid vesicles were prepared by sonication in 150 m*M* KCl, 20 m*M* $KH_2PO_4$, (or 150 m*M* NaCl, 20 m*M* $NaH_2PO_4$), pH 7.5, buffer and diluted 10 times in $Na^+$ (or $K^+$) buffer. $DiSC_2(3)$ was added to a final concentration of 2 μ*M*. In experiments for the estimation of plasma membrane potential, the potential-sensitive cyanine dye $DiSC_2(3)$ solution was added to the cell suspension (cell suspension medium was 150 m*M* KCl and 20 m*M* $KH_2PO_4$, pH 7.5) and incubated for 10–15 min at room temperature before data were collected. Depletion of cholesterol from 3T3 cell membranes was carried out by treatment with cyclodextrin [30].

#### *Time-Resolved Fluorescence Microscopy*

The experimental setup was a combination of a picosecond time-resolved fluorescence spectrometer and an inverted epifluorescence microscope described in detail earlier [27,28]. The time-resolved fluorescence setup consists of a mode-locked Nd:YAG laser, a rhodamine 6G dye laser, and a time-correlated, single-photon counting system. The temporal resolution of the setup is ~30 ps, and the spatial resolution is ~1 μm. Measurements require as less as ~100 fluorophore molecules in the observation volume. Cells loaded with cSNARF-1 were excited by 571-nm pulses, and fluorescence was collected beyond 600 nm by using a 600 nm high-pass filter. In the case of $DiSC_2(3)$ and Nile red the cells were excited at 575 nm and 571 nm, respectively, and the fluorescence was collected beyond 615 nm by using 630DF30 filter. For the single point measurements,

**Table I.** Parameters Obtained from Time-Resolved Fluorescence of the pH Probe SNARF-1 and the Estimated pH Values in Various Cell Types

| Cell Type | Sample | Lifetime (ns)[a] | | | Amplitudes[a] | | | Normalized Amplitude | pH Estimated by Normalized Amplitude[b] | Mean pH[c] |
|---|---|---|---|---|---|---|---|---|---|---|
| | | $\tau_1$ | $\tau_2$ | $\tau_3$ | $\alpha_1$ | $\alpha_2$ | $\alpha_3$ | $\alpha_1(\alpha_1 + \alpha_2)$ | | |
| 3T3[d] | Control | 0.25 | 1.24 | 2.98 | 0.40 | 0.47 | 0.12 | 0.45 | 6.77 | 6.75 ± 0.03 |
| | 550 μ*M* PEI[e] | 0.27 | 1.25 | 3.39 | 0.28 | 0.64 | 0.08 | 0.30 | 7.05 | 7.01 ± 0.05 |
| SF 9[f] | Control | 0.19 | 1.07 | 2.85 | 0.38 | 0.56 | 0.06 | 0.40 | 6.86 | 6.89 ± 0.07 |
| | 696 μ*M*PEI | 0.24 | 1.09 | 2.92 | 0.27 | 0.62 | 0.11 | 0.30 | 7.05 | 7.20 ± 0.10 |
| BY2[g] | Control | 0.42 | 1.27 | 3.39 | 0.53 | 0.42 | 0.05 | 0.56 | 6.59 | 6.55 ± 0.07 |
| | 638 μ*M*PEI | 0.44 | 1.27 | 3.28 | 0.50 | 0.45 | 0.05 | 0.53 | 6.63 | 6.65 ± 0.07 |
| *S. cerevisae*[h] | Control | 0.33 | 1.22 | 3.09 | 0.26 | 0.69 | 0.05 | 0.27 | 7.12 | 7.12 ± 0.03 |
| | 522 μ*M* PEI | 0.24 | 1.19 | 2.40 | 0.20 | 0.76 | 0.04 | 0.21 | 7.28 | 7.30 ± 0.05 |
| CHO[i] | Control | 0.29 | 1.21 | 2.81 | 0.35 | 0.54 | 0.11 | 0.39 | 6.89 | 6.86 ± 0.05 |
| | 139 μ*M* PEI | 0.29 | 1.16 | 2.71 | 0.32 | 0.55 | 0.13 | 0.37 | 6.91 | 6.88 ± 0.06 |
| | 550 μ*M* PEI | 0.26 | 1.19 | 2.85 | 0.30 | 0.60 | 0.10 | 0.33 | 7.00 | 7.03 ± 0.07 |
| | 1.39 m*M* PEI | 0.23 | 1.27 | 2.68 | 0.22 | 0.73 | 0.05 | 0.23 | 7.23 | 7.25 ± 0.06 |
| None | PBS (cell free control) | 0.48 | 1.32 | – | 0.23 | 0.77 | – | 0.23 | 7.23 | |
| | PBS + 139 μ*M* PEI | 0.49 | 1.33 | – | 0.21 | 0.79 | – | 0.21 | 7.28 | |
| | PBS + 1.39 m*M* PEI | 0.56 | 1.34 | – | 0.21 | 0.79 | – | 0.21 | 7.28 | |

[a] $\chi^2$ values were between 0.9 and 1.1 for all the data.
[b] This value corresponds to the typical data set (lifetimes and amplitudes) given. pH values were estimated from a standard curve similar to that given in Srivastava and Krishnamoorthy, 1997, Ref. 28].
[c] Estimated from measurements on different locations within a single cell or in many cells.
[d] $\sim 0.3 \times 10^5$ cells in 1 ml phosphate buffered saline, pH 7.5 (PBS).
[e] All the stated PEI concentrations are in terms of nitrogen content of PEI.
[f] $\sim 1.3 \times 10^6$ cells in 1 ml PBS.
[g] 200 μL of cell suspension in Murashige and Skoog salts with minimal organics (pH 5.8).
[h] 200 μL of cell suspension in PBS.
[i] $\sim 0.7 \times 10^6$ cells in 1 ml of PBS.

the laser beam was focused to ~1 μm within the cell at different locations. In case of the whole-cell measurements, the laser beam was defocused by placing a lens (25 cm focal length) before the objective lens. This arrangement could cover the entire area of a single cell. The instrument response function was estimated by the use of Oxonol VI, whose fluorescence lifetime is < 30 ps [28].

### *Data Analysis*

The observed fluorescence decay curves collected at the magic angle were analyzed by deconvoluting them with the instrument response function to get the intensity decay function (I(t)) as a sum of exponentials:

$$I(t) = \Sigma\alpha_i \exp(-t/\tau_i)\ i = 1\text{–}3 \qquad (1)$$

where $\alpha_i$ is the amplitude associated with the i-th fluorescence lifetime $\tau_i$ such that $\Sigma\alpha_i = 1$.

For the lifetime distribution the fluorescence intensity decay was fitted to a sum of N exponentials by the maximum entropy method (MEM) [31]. MEM begins with an initial condition in which the lifetimes are distributed in a particular range (say 10 ps–10 ns) that is covered by N exponentials (N = 100) with $\tau$ values equally spaced in log$\tau$ space. For this distribution the entropy S (Shannon-Jayne's entropy) and the reduced $\chi^2$ are calculated [31]:

$$S = -\Sigma\alpha_i \log \alpha_i \qquad (2)$$

Data analysis consisted of modifying $\alpha_i$ in each iteration such that minimization of $\chi^2$ and maximization of S occurred.

### *Estimation of Intracellular pH*

Fluorescence lifetime of the dual-emission pH probe cSNARF-1 was used to measure the intracellular pH. Under cell-free conditions, the fluorescence decay of cSNARF-1 follows a sum of two exponentials with lifetimes of ~0.3 ns($\tau_1$) and ~1.3 ns($\tau_2$), corresponding to protonated and deprotonated forms of the probe,respectively [28]. When the probe is present inside cells, a third lifetime component of ~3 ns($\tau_3$) is also seen. This component originates from probes bound to various macromolecules [28]. The pH inside cells was estimated from the amplitude ratio $\alpha_1/(\alpha_1 + \alpha_2)$ by using a standard curve obtained under cell-free conditions as described earlier [28]. Thus the presence of bound probe population does

not interfere with pH estimations, unlike the case in ratiometric intensity measurements [32].

*Estimation of Plasma Membrane Potential*

The membrane potential–sensing fluorescent probe $DiSC_2(3)$ was used to estimate change in membrane potential across cell membranes by measuring its fluorescence lifetime. The change in the relative amplitude ($\alpha_i$) of the free and bound components of the probe was used as a measure of membrane potential [33]. In lipid vesicles, membrane potential was created by the action of valinomycin (0.6 μg per mg of lipid) on the concentration gradient of $K^+$ across the membrane [34]. Because the concentration gradient (of both directions) was about 1 order of magnitude, the diffusion potential thus established is expected to be around 60 mV [33].

## RESULTS AND DISCUSSION

### Effect of PEI on Cell Membranes

It is generally accepted that transfection complexes enter the cell through endocytosis [3,24,25,35–37]. Transfection agents by virtue of their positive charge could be expected to interact with cell membranes that have net negative charge. Cationic detergents have been shown to interact with membranes [38,39]. PEI itself has been shown to interact with lipid membranes [40], lysosomal membranes [41] and to disrupt the outer membrane of gram-negative bacteria [42,43]. Hence it was of interest to check the effect of PEI on the membranes of the cells used in our work. Polarity-sensing florescent probe Nile red [44] was used in assessing the membrane heterogeneity [45,46]. Figure 1 shows fluorescence lifetime distributions, obtained by MEM, of Nile red in 3T3 cell membranes. The peak position and the width of lifetime distribution of Nile red have been earlier used in inferring the effect of membrane additives on the heterogeneity and polarity of membranes [30,45,46]. It can be seen that PEI has no significant effect on the lifetime distribution of Nile red. The concentration (by total N) of PEI (0.7 m*M*) used in this experiment is significantly higher than the concentration (60–400 μ*M*) used in transfection protocols [5,47–49]. Hence we could conclude that the plasma membrane is largely unaffected even by the presence of very high concentrations of PEI as monitored by Nile red. In contrast to the observations with PEI, depletion of cholesterol by treatment with cyclodextrin led to significant decrease in the width of lifetime distribution similar to our earlier observations [30]. Decrease in the width of lifetime distribution with decrease in cholesterol content has been shown in lipid membranes also [46].

### Effect of PEI on Intracellular pH

We have used the technique of time-resolved fluorescence microscopy to estimate intracellular pH using the pH dependence of fluorescence decay kinetics of SNARF-1. SNARF-1 is a dual emission pH probe [28,29], and hence the relative amplitudes of the lifetimes corresponding to acidic and basic forms can be used for the estimation of pH [28]. It was earlier [28] demonstrated that time-resolved fluorescence measurements were superior to ratiometric intensity measurements often used for the determination of pH optically. It was also shown that SNARF-1 exhibits a significant amount of binding to cell components. To correct for the probe binding within the cell and thus estimate the pH accurately, it was important to resolve the bound and free forms. This can be done very effectively by time-resolved fluorescence because the bound populations and the free forms have very different fluorescence lifetimes. (The free probe has a lifetime of 0.25–0.4 ns and 1.1–1.3 ns (corresponding to acidic and basic forms, respectively),

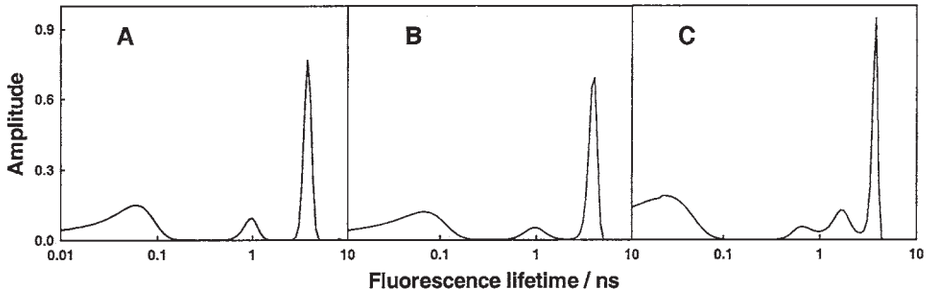


**Fig. 1.** Lifetime distribution of Nile red in Swiss 3T3 fibroblast membranes. (A) Control cells (peak position and width of distribution are 3.79 ns, and 0.98 ns, respectively). (B) PEI added to ~30,000 cells (0.7 m*M* PEI, in 1 ml of PBS) (peak position and width of distribution are 3.88 ns and 1.06 ns, respectively). (C) Cyclodextrin-treated cells (peak position and width of distribution are 3.76 ns and 0.52 ns, respectively).

whereas all the bound populations can be represented by a single lifetime of ~ 3 ns [28]). Such a correction is nontrivial in ratiometric intensity measurements. Thus this method allows us to monitor small changes in intracellular pH very precisely within a single cell.

Table I lists the dynamic fluorescence parameters obtained from analysis of fluorescence decay of SNARF-1 in the various cell types used and the pH values estimated from these parameters. As mentioned before, the pH was estimated from the relative amplitudes of the protonated ($\alpha_1$) and deprotonated ($\alpha_2$) free forms of SNARF-1. Although the pH values given in Table I are similar to those estimated by others [32,50], the small differences observed between the two types of estimations could be due to the complications introduced by bound probes in methods based on fluorescence spectra [32]. Also, the slightly lower values of pH estimated by our method when compared to other estimations [32,50] could be due to the contribution of acidic compartments such as endosomes and Golgi in our measurements. Several points could be noted from our data (Table I): (i) The intracellular pH increases when the cells are treated with PEI [the increase in pH was inferred from the decrease in the value of $\alpha_1$ and the corresponding decrease in the normalized amplitude $\alpha_1/\alpha_1 + \alpha_2$)]; (ii) the increase in the pH is cell-type dependent and varies in the range of 0.1–0.4. The extent of increase in pH was beyond the level of variations observed from cell to cell (see the last column in Table I); (iii) the PEI-induced increase in cell pH was dose dependent (Table I, CHO cells); and (iv) there is about 3–13% bound population and the extent of probe binding is cell-type dependent.

Intracellular pH measurements were carried out in two ways: (i) single point measurements by parking a focused (~1 μm) exciting laser beam at various locations within a single cell and (ii) whole-cell measurements by using a diffused laser beam so as to cover an entire cell. In the first type of measurement, many observations were made within a single cell. The last column in Table I gives the mean and standard deviation of pH measurements. These values refers to a number (about 10) of either point measurements or whole-cell measurements carried out on 7–10 single cells one at a time. It was seen that the pH changes occurred within ~10 min after adding PEI to the cell suspension and remained stable thereafter (data not shown). The observed increase in intracellular pH was dose dependent (Table I) in the range of 0.14–1.4 m*M* of PEI nitrogen. It should be mentioned that the increase in intracellular pH occurred even when the concentration of PEI was in the range of a few hundred micromoles, which is used normally in transfection procedures [5,47–49].

To check whether the observed increase in the intracellular pH is caused by the internalization of PEI or by a trivial effect of increase in the medium pH by the addition of PEI, we estimated the effect of PEI on the pH of the medium under cell-free conditions. In these measurements also, the fluorescence decay kinetics of SNARF-1 (free acid) was used for the estimation of pH. It was found that the effect of PEI on the pH of the medium was significantly smaller compared to the changes in intracellular pH (Table I). Also, a small increase in the medium pH would have caused similar increase in intracellular pH for all the cell types by PEI, contrary to observations.

As mentioned earlier it has been shown [24–26] that free PEI in the medium gets internalized by endocytosis. Confocal images of the cell interior in the presence of fluorescence-labeled free PEI were identical to those of cells treated with PEI-DNA complex [24,25], showing that the accessible regions of free PEI and the complex are very similar. How does the internalization of PEI cause the increase in the cytoplasmic pH? PEI has a large number of amine groups (every third atom is an amino nitrogen). The acid titration curve of PEI shows a broad continuum of pK values [4]. PEI has a highly branched structure that can ensnare the DNA and has a substantial buffering capacity at virtually any pH [4]. It is likely that this property of PEI accounts for its efficacy as a transfection agent. It has been hypothesized that its high buffering capacity helps protect the DNA during intracellular trafficking [5,49]. We believe that this property causes the observed increase in intracellular pH. Having a large number of protonable amine groups, PEI could soak up the protons in the endocytic vesicle, increasing the pH and thereby inhibiting the endosomal nucleases that have an acid optimal pH and thus protecting the DNA. Subsequently, PEI could swell as a result of internal charge repulsion between the closely placed protonated amine groups. Although the exact mechanism of release of the complex from endosomes is not known, there are suggestions indicating that the release could occur because of osmotic swelling and rupture of endosomes induced by counter ion influx [5,49]. Such a mechanism gets support from the observed decrease in the level of reporter gene expression mediated by PEI in the presence of proton pump inhibitors [49]. It is likely that PEI taken up by endocytosis is released from endosomes into the cytoplasm. Evidence for such a phenomenon has been recently seen in fluorescence correlation spectroscopy experiments (J. P. Clamme, G. Krishnamoorthy, and Y. Mely, unpublished observation). Although the mechanism involving the release of PEI-DNA complex is essential for the action of any transfection complex, it still remains hypothetical. The

intracellular pH is generally regulated by plasma membrane $Na^+/H^+$ exchangers. Hence, one could also visualize a mechanism wherein inhibition of $Na^+/H^+$ exchanger by PEI causes the dysregulation of cytoplasmic pH. In this connection it is interesting to note that pH regulation by $Na^+/H^+$ exchanger requires phosphatidylinositol 4,5-diphosphate [51]. Sequestration of phosphatidylinositol 4,5-diphosphate by PEI could have caused the observed pH dysregulation.

Will the observed increase in intracellular pH lead to dysfunction of cells? Although it appears that the observed extent of increase in intracellular pH is quite small, we believe that these changes are manifestations of significant cell perturbations. Similar dysregulation of cellular pH has been suggested as a cause for cell death in some cases [52]. Godbey *et al.* [20] have shown that free PEI treatment causes two distinct types of cell deaths. The first type of cell death is due to membrane destabilization [20,21], which is fast, and the second mechanism is slower and probably due to the effect of internalized PEI [20]. Further, the first type is largely absent in the case of low molecular weight PEI similar to that used in our studies. Our observation of insignificant changes in membrane heterogeneity and polarity (Fig. 1) is consistent with this model. Thus it may be speculated that the dysregulation of cytoplasmic pH and plasma membrane potential (see below) are among the causative agents for the slow cell death observed in earlier studies [20,21].

### Effect of PEI on Plasma Membrane Potential

Electrical potential across plasma membranes is another important cellular parameter. A variety of fluorescence probes have been used for estimating membrane potential in cells and artificial systems (see, for example, Refs. 33,53–56]. In this work we have used a cyanine probe $DiSC_2(3)$ for estimating the effect of PEI on plasma membrane potential in single cells of *S. cerevisae* and Swiss 3T3 fibroblasts. One of us had shown earlier, by time-resolved fluorescence, that the sensitivity of fluorescence intensity of cyanine probes to changes in membrane potential arises from the change in their level of membrane partitioning [33]. The levels of populations of free and membrane-bound probes could be estimated from the amplitudes associated with their fluorescence lifetimes [33].

To validate the use of $DiSC_2(3)$ in cells we tested this probe in lipid vesicles. Table II lists the parameters obtained from fluorescence decay kinetics of $DiSC_2(3)$ in soybean phospholipid membranes. Membrane potential of either polarity was generated in these membranes by $K^+$ diffusion potential by the action of $K^+$ ionophore valinomycin [33,57] (see Methods section). Fluorescence decay kinetics of $DiSC_2(3)$ followed a sum of three exponentials in the presence of vesicle membranes (Table II). The shortest lifetime ($\tau_1 \sim 0.1$ ns) represents the free probe and the other two longer lifetimes ($\tau_2$ and $\tau_3$) correspond to bound populations. These two populations could represent probes bound at two different locations such as interface and interior [58]. Creation of negative-inside membrane potential results in an increase in the level of binding of positively charged $DiSC_2(3)$ (as shown by increase in $\alpha_2$ and $\alpha_3$) and a corresponding decrease in the free population ($\alpha_1$) (Table II). An opposite effect was observed when the sign of membrane potential was reversed (Table II). Although these observations are similar to those observed with a similar probe $DiOC_2(5)$ [33], the magnitude of changes are significantly larger in the case of $DiSC_2(3)$. This could be due to shorter aliphatic chain in the case of $DiSC_2(3)$ compared to $DiOC_2(5)$ and hence more even distribution between the aqueous and membrane phases.

Table III shows the effect PEI on the plasma membrane potential in *S. cerevisae* and Swiss 3T3 fibroblast cells. The extent of membrane potential was inferred from the difference in the level of free aqueous population of $DiSC_2(3)$ (represented by $\alpha_1$) in the absence and in the presence of valinomycin. Unlike in the case of vesicle samples mentioned above, addition of valinomycin in a $K^+$ medium abolishes the (negative-inside) membrane potential in cells [56]. The abolition of membrane potential by valinomycin is accompanied by an increase in the value of $\alpha_1$. This represents an increase in the level of free population of $DiSC_2(3)$ caused by a shift of the membrane-water partition of $DiSC_2(3)$ toward the aqueous phase. [In the absence of valinomycin the partition is more favored toward the membrane because of the presence of membrane potential. This negative-inside potential favors the binding of positively charged $DiSC_2(3)$]. It can be seen that the level of valinomycin-induced increase in $\alpha_1$ ($\Delta\alpha_1$, last column in Table III) decreases with the increase in the concentration of PEI. A situation in which $\Delta\alpha_1$ approaches zero could be taken as an indication for the absence of membrane potential. Whereas *S. cerevisae* cells required very high concentrations of PEI for depolarization, 3T3 fibroblast cells were depolarized at PEI concentrations of 290 $\mu M$, which lies in the range used in transfection protocols [5,47–49]. This effect of PEI on the plasma membrane potential could be the result of either a general mechanism of membrane disorganization or a specific effect of inhibition of plasma membrane ion pumps responsible for the

**Table II.** Parameters Obtained from Time-Resolved Fluorescence of the Membrane-Potential Probe $DiSC_2(3)$ in Soybean Phospholipid (SBPL) Vesicles

| Sample | Membrane Potential[a] | Lifetime (ns)[b] | | | Amplitude[b] | | | Mean lifetime[b,c] $\tau_m$ (ns) | $\chi^2$ | Mean Amplitude[d] |
|---|---|---|---|---|---|---|---|---|---|---|
| | | $\tau_1$ | $\tau_2$ | $\tau_3$ | $\alpha_1$ | $\alpha_2$ | $\alpha_3$ | | | $\alpha_1$ |
| SBPL vesicles | 0 | 0.07 | 0.79 | 1.29 | 0.37 | 0.39 | 0.25 | 0.65 | 0.99 | 0.35 ± 0.04 |
| | +ve inside | 0.07 | 0.79 | 1.29 | 0.47 | 0.37 | 0.16 | 0.54 | 0.99 | 0.42 ± 0.06 |
| SBPL vesicles | 0 | 0.12 | 0.75 | 1.21 | 0.23 | 0.43 | 0.34 | 0.76 | 0.90 | 0.26 ± 0.09 |
| | −ve inside | 0.12 | 0.75 | 1.21 | 0.06 | 0.56 | 0.38 | 0.88 | 0.90 | 0.12 ± 0.09 |

[a] Membrane potential was created by valinomycin-induced $K^+$ transport (see Methods section).
[b] Typical values obtained from time-resolved fluorescence decay of $DiSC_2(3)$ in SBPL vesicles (lipid concentration is 0.7 mg/ml).
[c] Mean lifetime $\tau_m = \Sigma\alpha_i\tau_i$.
[d] Mean value from a large number of estimations.

**Table III.** Parameters Obtained from Time-Resolved Fluorescence Decay of $DiSC_2(3)$ in *S. cerevisae* and Swiss 3T3 Fibroblast Cells

| Cell type | Sample | Valinomycin | Lifetime (ns)[a] | | | Amplitudes[a] | | | $\Delta\alpha_1$[b] | Mean Lifetime[a] $\tau_m$ (ns) | $\chi^{2a}$ | Mean Amplitude[c] $\alpha_1$ | Mean $\Delta\alpha_1$[c] |
|---|---|---|---|---|---|---|---|---|---|---|---|---|---|
| | | | $\tau_1$ | $\tau_2$ | $\tau_3$ | $\alpha_1$ | $\alpha_2$ | $\alpha_3$ | | | | | |
| *S. cerevisae*[d] | Control | − | 0.13 | 0.92 | 2.38 | 0.59 | 0.30 | 0.11 | 0.08 | 0.62 | 0.95 | 0.59 ± 0.03 | 0.08 |
| | | + | 0.12 | 0.89 | 2.33 | 0.67 | 0.24 | 0.09 | | 0.50 | 1.10 | 0.67 ± 0.02 | |
| | 139.2 μ*M* PEI | − | 0.13 | 0.96 | 2.45 | 0.53 | 0.35 | 0.12 | 0.06 | 0.71 | 0.93 | 0.53 ± 0.03 | 0.06 |
| | | + | 0.13 | 0.84 | 2.37 | 0.59 | 0.30 | 0.11 | | 0.60 | 1.19 | 0.59 ± 0.03 | |
| | 1.39 m*M* PEI | − | 0.13 | 0.90 | 2.52 | 0.49 | 0.39 | 0.12 | 0.04 | 0.72 | 0.83 | 0.49 ± 0.03 | 0.05 |
| | | + | 0.12 | 0.96 | 2.67 | 0.53 | 0.36 | 0.11 | | 0.72 | 1.02 | 0.54 ± 0.04 | |
| | 13.9 m*M* PEI | − | 0.19 | 1.06 | 3.34 | 0.44 | 0.44 | 0.12 | 0.00 | 0.88 | 1.03 | 0.44 ± 0.03 | −0.01 |
| | | + | 0.13 | 1.04 | 3.50 | 0.44 | 0.42 | 0.14 | | 0.97 | 0.89 | 0.43 ± 0.04 | |
| 3T3[e] | Control | − | 0.23 | 0.92 | 2.79 | 0.42 | 0.45 | 0.13 | 0.05 | 0.87 | 1.00 | 0.43 ± 0.04 | 0.06 |
| | | + | 0.16 | 0.90 | 2.64 | 0.47 | 0.40 | 0.13 | | 0.77 | 1.10 | 0.49 ± 0.04 | |
| | 29 μ*M* PEI | − | 0.18 | 0.82 | 2.62 | 0.42 | 0.46 | 0.12 | 0.01 | 0.76 | 0.92 | 0.42 ± 0.05 | 0.02 |
| | | + | 0.16 | 0.93 | 2.49 | 0.43 | 0.43 | 0.14 | | 0.82 | 0.92 | 0.44 ± 0.07 | |
| | 290 μ*M* PEI | − | 0.23 | 0.83 | 2.72 | 0.45 | 0.45 | 0.10 | 0.00 | 0.76 | 1.05 | 0.45 ± 0.03 | 0.00 |
| | | + | 0.18 | 0.91 | 2.69 | 0.45 | 0.44 | 0.11 | | 0.78 | 0.86 | 0.45 ± 0.03 | |
| | 2.9 m*M* PEI | − | 0.30 | 0.95 | 2.69 | 0.44 | 0.44 | 0.12 | −0.03 | 0.87 | 1.09 | 0.44 ± 0.04 | 0.01 |
| | | + | 0.20 | 0.93 | 2.67 | 0.41 | 0.49 | 0.10 | | 0.81 | 0.89 | 0.45 ± 0.10 | |

[a] Typical values obtained from time-resolved fluorescence decay of $DiSC_2(3)$ in cells.
[b] $\Delta\alpha_1$ refers to the difference between $\alpha_1$ in the presence and in the absence of valinomycin.
[c] The mean values of $\alpha_1$ and $\Delta\alpha_1$ correspond to a large number of measurements.
[d] The sample had 2 μ*M* $DiSC_2(3)$, the valinomycin was added to a final concentration of 20 μ*M*, and the PEI was added to $\sim 3.0 \times 10^6$ cells in 150 μL of cell suspension.
[e] The sample had 7 μ*M* $DiSC_2(3)$, the valinomycin was added to a final concentration of 11 μ*M*, and the PEI was added to $\sim 0.3 \times 10^5$ cells in a dish having 1 ml of buffer.

generation of membrane potential. However, the absence of any discernable effect on cell membranes by PEI (Fig. 1) does not favor the former mechanism. In the case of *S. cerevisae* cells, addition of PEI (in the absence of valinomycin) caused a decrease in the value of $\alpha_1$ (Table III). This could be due to shift in the partition equilibrium caused by the presence of PEI. However, because we estimate the level of membrane potential by the valinomycin-induced increase in $\alpha_1$, our conclusions are largely unaffected.

## CONCLUSIONS

Treatment of cells with free PEI concentrations in the range of that in mixtures of DNA and PEI used for transfection led to (i) significant increase in intracellular pH probably resulting from dysfunction of pH regulation mechanism(s) and (ii) depolarization of plasma membrane potential. It is likely that these changes result in significant alteration of various cellular functions and contribute to the cytotoxic effects of PEI. Transfection could

be thought of as a process of invasion of cells by external agents. Normal and healthy cells could be expected to offer resistance to such an invasion. Accordingly, the ability of free PEI to alter several cellular functions may reduce the cellular resistance to the transfecting PEI/DNA complexes and thus explain the high efficiency of PEI compared to many other DNA condensing agents. In this respect, free PEI in mixtures of DNA and PEI might be considered as a cofactor for transfection.

## REFERENCES


1. D. J. Jolly, J. K. Yee, and T. Friedmann (1987) High-efficiency gene transfer into cells. *Methods Enzymol.* **149**, 10–25.
2. J. P. Behr (1993) Synthetic gene transfer vectors. *Account. Chem. Res.* **26**, 274–278.
3. J. Zabner, A. J. Fasbender, T. Moninger, K. A. Poellinger, and M. J. Welsh (1995) Cellular and molecular barriers to gene transfer by a cationic lipid. *J. Biol. Chem.* **270**, 18997–19007.
4. M. X. Tang and F. C. Szoka (1997) The influence of polymer structure on the interactions of cationic polymers with DNA and morphology of the resulting complexes. *Gene Ther.* **4**, 823–832.
5. O. Boussif, F. Lezoualc'h, M. A. Zanta, M. D. Mergny, D. Scherman, B. Demeneix, and J. P. Behr (1995) A versatile vector for gene and oligonucleotide transfer into cells in culture and in vivo: Polyethyleneimine. *Proc. Natl. Acad. Sci. USA* **92**, 7297–7301.
6. O. Boussif, M. A. Zanta, and J. P. Behr (1996) Optimized galenics improve in vitro gene transfer with cationic molecules up to 1000-fold. *Gene Ther.* **3**, 1074–1080.
7. R. Kircheis, A. Kichler, G. Wallner, M. Kursa, M. Ogris, T. Felzmann, M. Buchberger, and E. Wagner (1997) Coupling of cell-binding ligands to polyethyleneimine for targeted gene delivery. *Gene Ther.* **4**, 409–418.
8. J. S. Remy, D. Goula, A. M. Steffan, M. A. Zanta, O. Boussif, J. P. Behr, and B. Demeneix (1998) in A. V. Kabanov, P. L. Felgner, and L. W. Seymour (Eds.) *Self Assembling Complexes for Gene Delivery*, Wiley, Chichester, pp. 135–148.
9. B. Abdallah, A. Hassan, C. Benoist, D. Goula, J. P. Behr, and B. A. Demeneix (1996) A powerful nonviral vector for in vivo gene transfer into the adult mammalian brain: Polyethylenimine. *Hum. Gene Ther.* **7**, 1947–1954.
10. D. Goula, J. S. Remy, P. Erbacher, M. Wasowicz, G. Levi, B. Abdallah, and B. A. Demeneix (1998) Size, diffusibility and transfection performance of linear PEI/DNA complexes in the mouse central nervous system. *Gene Ther.* **5**, 712–717.
11. D. Goula, C. Benoist, S. Mantero, G. Merlo, G. Levi, and B. A. Demeneix (1998) Polyethylenimine-based intravenous delivery of transgenes to mouse lung. *Gene Ther.* **5**, 1291–1295.
12. E. Dauty, J. S. Remy, T. Blessing, and J. P. Behr (2001) Dimerizable cationic detergents with a low CMC condense plasmid DNA into nanometric particles and transfect cells in culture. *J. Amer. Chem. Soc.* **123**, 9227–9234.
13. T. Bettinger, J. S. Remy, and P. Erbacher (1999) Size reduction of galactosylated PEI/DNA complexes improves lectin-mediated gene transfer into hepatocytes. *Bioconjug. Chem.* **10**, 558–561.
14. S. Han, R. I. Mahato, and S. W. Kim (2001) Water-soluble lipopolymer for gene delivery. *Bioconjug. Chem.* **12**, 337–345.
15. J. Haensler and F. C. Szoka (1993) Polyamidoamine cascade polymers mediate efficient transfection of cells in culture. *Bioconjug. Chem.* **4**, 372–379.
16. P. Midoux and M. Monsigny (1999) Efficient gene transfer by histidylated polylysine/pDNA complexes. *Bioconjug. Chem.* **10**, 406–411.
17. V. Vijayanathan, T. Thomas, A. Shirahata, and T. J. Thomas (2001) DNA condensation by polyamines: A laser light scattering study of structural effects. *Biochemistry* **40**, 13644–13651.
18. P. Erbacher, S. Zou, T. Bettinger, A. M. Steffan, and J. S. Remy (1998) Chitosan-based vector/DNA complexes for gene delivery: Biophysical characteristics and transfection ability. *Pharm. Res.* **15**, 1332–1339.
19. M. A. Zanta, O. Boussif, A. Adib, and J. P. Behr (1997) In vitro gene delivery to hepatocytes with galactosylated polyethylenimine. *Bioconjug. Chem.* **8**, 839–844.
20. W. T. Godbey, K. K. Wu, and A. G. Mikos (2001) Poly(ethyleneimine)-mediated gene delivery affects endothelial cell function and viability. *Biomaterials* **22**, 471–480.
21. D. Fischer, T. Bieber, Y. Li, H-P. Elsasser, and T. Kissel (1999) A novel non-viral vector for DNA delivery based on low molecular weight, branched polyethyleneimine: Effect of molecular weight on transfection efficiency and cytotoxicity. *Pharmaceut. Res.* **16**, 1273–1279.
22. D. Finsinger, J. S. Remy, P. Erbacher, C. Koch, and C. Plank (2000) Protective copolymers for nonviral gene vectors: Synthesis, vector characterization and application in gene delivery. *Gene Ther.* **7**, 1183–1192.
23. J. P. Clamme, J. Azoulay, and Y. Mély (2003) Monitoring of the formation and dissociation of polyethyleneimine/DNA complexes by two photon fluorescence correlation spectroscopy. *Biophys J.* In press.
24. W. T. Godbey, K. K. Wu, and A. G. Mikos (1999) Tracking the intracellular path of poly(ethylenimine)/DNA complexes for gene delivery. *Proc. Natl. Acad. Sci. USA* **96**, 5177–5181.
25. A. Remy-Kristensen, J. P. Clamme, C. Vuilleumier, J. G. Kuhry, and Y. Mely (2001) Role of endocytosis in the transfection of L929 fibroblasts by polyethylenimine/DNA complexes. *Biochim. Biophys. Acta* **1514**, 21–32.
26. M. Lecocq, S. Wattiaux-De Coninck, N. Laurent, R. Wattiaux, and M. Jadot (2000) Uptake and intracellular fate of polyethyleneimine in vivo. *Biochem. Biophys. Res. Commun.* **278**, 414–418.
27. A. Srivastava and G. Krishnamoorthy (1997) Cell type and spatial location dependence of cytoplasmic viscosity measured by time-resolved fluorescence microscopy. *Arch. Biochem. Biophys.* **340**, 159–167.
28. A. Srivastava and G. Krishnamoorthy (1997) Time-resolved fluorescence microscopy could correct for probe binding while estimating intracellular pH. *Anal. Biochem.* **249**, 140–146.
29. A. Srivastava and G. Krishnamoorthy (1997) Intracellular dynamics seen through time-resolved fluorescence microscopy. *Curr. Sci.* **72**, 835–845.
30. G. Krishnamoorthy and Ira (2001) Fluorescence lifetime distribution in characterizing membrane microheterogeneity. *J. Fluoresc.* **11**, 247–253.
31. R. Swaminathan and N. Periasamy (1996) Analysis of fluorescence decay by the maximum entropy method: Influence of noise and analysis parameters on the width of the distribution of lifetimes. *Proc. Indian Acad. Sci. (Chem. Sci.)* **108**, 39–49.
32. O. Seksek and J. Bolard (1996) Nuclear pH gradient in mammalian cells revealed by laser microspectrofluorimetry. *J. Cell Sci.* **109**, 257–262.
33. T. K. Das, N. Periasamy, and G. Krishnamoorthy (1993) Mechanism of response of potential sensitive dyes studied by time-resolved fluorescence. *Biophys. J.* **64**, 1122–1132.
34. G. Krishnamoorthy (1986) Temperature jump as a new technique to study the kinetics of fast transport of protons across membranes. *Biochemistry* **25**, 6666–6671.
35. X. Gao and L. Huang (1995) Cationic liposome-mediated gene transfer. *Gene Ther.* **2**, 710–722.
36. E. Tomlinson and A. P. Rolland (1996) Controllable gene therapy: Pharmaceutics of non-viral gene delivery systems. *J. Control. Release* **39**, 357–372.
37. C. W. Pouton, P. Lucas, B. J. Thomas, A. N. Uduehi, D. A. Milroy, and S. H. Moss (1998) Polycation-DNA complexes for gene delivery: A comparison of the biopharmaceutical properties of

cationic polypeptides and cationic lipids. *J. Control. Release* **53**, 289–299.
38. J. P. Clamme, S. Bernacchi, C. Vuilleumier, G. Duportail, and Y. Mely (2000) Gene transfer by cationic surfactants is essentially limited by the trapping of the surfactant/DNA complexes onto the cell membrane: A fluorescence investigation. *Biochim. Biophys. Acta* **1467**, 347–361.
39. D. Lleres, E. Dauty, J. P. Behr, Y. Mely, and G. Duportail (2001) DNA condensation by an oxidizable cationic detergent: Interactions with lipid vesicles. *Chem. Phys. Lipids* **111**, 59–71.
40. N. Oku, N. Yamaguchi, N. Yamaguchi, S. Shibamoto, F. Ito, and M. Nango (1986) The fusogenic effect of synthetic polycations on negatively charged lipid bilayers. *J. Biochem.* **100**, 935–44.
41. A. R. Klemm, D. Young, and J. B. Lloyd (1998) Effects of polyethyleneimine on endocytosis and lysosome stability. *Biochem. Pharmacol.* **56**, 41–46.
42. I. M. Helander, K. Latva-Kala, and K. Lounatmaa (1998) Permeabilizing action of polyethyleneimine on *Salmonella typhimurium* involves disruption of the outer membrane and interactions with lipopolysaccharide. *Microbiology* **144**, 385–390.
43. I. M. Helander, H. L. Alakomi, K. Latva-Kala, and P. Koski (1997) Polyethyleneimine is an effective permeabilizer of gram-negative bacteria. *Microbiology* **143**, 3193–3139.
44. G. B. Dutt, S. Doraiswamy, N. Periasamy, and B. Venkatraman (1990) Rotational reorientation dynamics of polar dye molecular probes by picosecond laser spectroscopic technique. *J. Chem. Phys.* **93**, 8498–8513.
45. Ira and G. Krishnamoorthy (1998) Probing the dynamics of planar supported membranes by Nile red fluorescence lifetime distribution. *Biochim. Biophys. Acta* **1414**, 255–259.
46. Ira and G. Krishnamoorthy (2001) Probing the link between proton transport and water-content in lipid membranes. *J. Phys. Chem. B* **105**, 1484–1488.
47. P. Erbacher, T. Bettinger, P. Belguise-Valladier, S. Zou, J. L. Coll, J. P. Behr, and J. S. Remy (1999) Transfection and physical properties of various saccharide, poly(ethylene glycol), and antibody-derivatized polyethylenimines (PEI). *J. Gene Med.* **1**, 210–222.
48. M. Ogris, P. Steinlein, M. Kursa, K. Mechtler, R. Kircheis, and E. Wagner (1998) The size of DNA/transferrin-PEI complexes is an important factor for gene expression in cultured cells. *Gene Ther.* **5**, 1425–1433.
49. A. Kichler, C. Leborgne, E. Coeytaux, and O. Danos (2001) Polyethylenimine-mediated gene delivery: A mechanistic study. *J. Gene Med.* **3**, 135–144.
50. J. Llopis, J. M. McCaffery, A. Miyawaki, M. G. Farquhar, and R. Y. Tsien (1998) Measurement of cytosolic, mitochondrial, and Golgi pH in single living cells with green fluorescent proteins. *Proc. Natl. Acad. Sci. USA* **95**, 6803–6808.
51. O. Aharonovitz, H. C. Zaun, T. Balla, J. D. York, J. Orlowski, and S. Grinstein (2000) Intracellular pH regulation by $Na^+/H^+$ exchange requires phosphatidylinositol 4,5-bisphosphate. *J. Cell Biol.* **150**, 213–224.
52. S. Matsuyama and J. C. Reed (2000) Mitochondria-dependent apoptosis and cellular pH regulation. *Cell Death Differn.* **7**, 1155–1165.
53. A. S. Waggoner (1979) Dye indicators of membrane potential. *Annu. Rev. Biophys. Bioeng.* **8**, 47–68.
54. L. M. Loew (1991) in R. J. Cherry (Ed.) *New Techniques of Optical Microscopy and Microspectroscopy*, Macmillan, London, pp. 255–272.
55. W. Y. Kao, C. E. Davis, Y. I. Kim, and J. M. Beach (2001) Fluorescence emission spectral shift measurements of membrane potential in single cells. *Biophys. J.* **81**, 1163–1170.
56. D. Gaskova, B. Brodska, P. Herman, J. Vecer, J. Malinsky, K. Sigler, O. Benada, and J. Plasek (1998) Fluorescent probing of membrane potential in walled cells: DiS-$C_3$(3) assay in *Saccharomyces cerevisae. Yeast* **14**, 1189–1197.
57. I. Ahmed and G. Krishnamoorthy (1990) Enhancement of transmembrane proton conductivity of protonophores by membrane-permeant cations. *Biochim. Biophys. Acta* **1024**, 298–306.
58. M. M. G. Krishna and N. Periasamy (1998) Fluorescence of organic dyes in lipid membranes: Site of solubilization and effects of viscosity and refractive index on lifetimes. *J. Fluoresc.* **8**, 81–91.